Journal of Plant Physiology **166** (2009) 1624—1636

Available online at www.sciencedirect.com

ScienceDirect

JOURNAL OF PLANT PHYSIOLOGY

www.elsevier.de/jplph

Epigenetic characterization of the vegetative and floral stages of azalea buds: Dynamics of DNA methylation and histone H4 acetylation

Mónica Meijón[a,b], Luis Valledor[a,b], Estrella Santamaría[a,b], Pilar S. Testillano[d], M[a] Carmen Risueño[d], Roberto Rodríguez[a,b], Isabel Feito[c], María Jesús Cañal[a,b,*]

[a]*Laboratorio de Fisiología Vegetal, Dpto. B.O.S., Facultad de Biología, Universidad de Oviedo, C/Cat. Rodrigo Uria s/n, E-33071, Oviedo, Asturias, Spain*
[b]*Instituto de Biotecnología de Asturias (Associated with CSIC), Edificio Santiago Gascón, C/ Fernando Bongera s/n, E-33006 Oviedo, Asturias, Spain*
[c]*SERIDA, Servicio Regional de Investigación Desarrollo Agroalimentario, Finca ''La Mata'', Apdo 13, E-33820 Grado, Asturias, Spain*
[d]*Desarrollo en plantas y arquitectura nuclear, Centro de Investigaciones Biológicas CIB-CSIC, Ramiro Maeztu 9, E-28040 Madrid, Spain*

Received 9 January 2009; received in revised form 7 April 2009; accepted 8 April 2009

KEYWORDS
Chromatin configuration;
Epigenetic code;
Immunocyto-chemistry;
Phase change;
Plant development

Summary

Floral induction in plants is achieved through a complex genetic network and regulated by multiple environmental and endogenous cues. Epigenetic control is determinative in plants for coordinating the switch to flowering under favorable environmental conditions and achieving reproductive success. Global DNA methylation, whose increase is associated with heterochromatinization-cell differentiation, and histone H4 acetylation, which is linked to euchromatin, were analyzed in vegetative and floral buds of azalea in order to study the involvement of epigenetic mechanisms in the floral development of woody plants. The results showed an increase of DNA methylation in floral buds in contrast to the decrease observed for acetylated H4 (AcH4) levels. In addition, when the distributions of 5-mdC and AcH4 in vegetative and floral buds of azalea were analyzed by immunodetection, opposite patterns in their distribution were revealed and confirmed the existence of different cell types in the shoot apical meristem with varying degrees of differentiation.

*Corresponding author at: Laboratorio de Fisiología Vegetal, Dpto. B.O.S., Facultad de Biología, Universidad de Oviedo, C/Cat. Rodrigo Uria s/n, E-33071, Oviedo, Asturias, Spain. Tel.: +34 985 104 799; fax: +34 985 104 867.
E-mail address: mjcanal@uniovi.es (M.J. Cañal).

0176-1617/$ - see front matter © 2009 Elsevier GmbH. All rights reserved.
doi:10.1016/j.jplph.2009.04.014

Introduction

Azalea japonica forms a small part of the large genus *Rhododendron* L. (*Ericaceae*), which contains approximately 1000 described species and thousands of commercial hybrids with different flower morphotypes. In the ornamental plant industry, azalea production represents a major cultivation expansion; floral quality, in these species, is fundamental for their commercial success. The application of various chemical compounds such as plant growth regulators (PGRs) offer the opportunity to advance and/or enhance flowering depending on the species and timing of application, although the response of different cultivars is highly variable and not all chemicals guarantee effective control (Meijón et al., 2009).

For the ornamental industry, it is crucial to regulate the timing of flowering in azalea. However, each cultivar has specific temperature and photoperiod requirements (Bodson, 1983). The transition from the vegetative to reproductive state is the most dramatic change during plant development. The regulation of this essential plant process is achieved by a complex genetic network that monitors the developmental state of the plants as well as environmental conditions such as light and temperature (Blázquez and Weigel, 2000; Araki, 2001; Henderson and Dean, 2004). Genetic analysis of flowering-time mutants in *Arabidopsis* have allowed the identification of 80 genes placed in multiple genetic pathways that control floral transition (Blázquez and Weigel, 2000; Araki, 2001). The switch to flowering involves the coordination of the perception of environment (day length, light conditions and temperature) with endogenous factors such as developmental status and age. This coordination is decisive for reproductive success in plants, and several studies have demonstrated its correlation with epigenetic mechanisms such as DNA methylation and histone modification (Henderson and Dean, 2004; Dennis and Peacock, 2007).

Transitions between different developmental phases in shoot apical meristem (SAM) involve changes in the pattern of cellular differentiation and organ formation. SAM cells are organized at different levels; the central cells remain pluripotent, while cells in the periphery contribute to organ formation and eventually differentiate (Jacqmard et al., 2003; Tooke and Battey, 2003). This zoning is established during vegetative development of the plant. However, DNA replication patterns are extensively changed during floral transition, the cells of the central zone start to divide at a high frequency, and the zonation is lost (Zluvova et al., 2001). These changes in SAM are included among other processes genetically regulated by epigenetic mechanisms (Zluvova et al., 2001; Ruiz-García et al., 2005; Vijayraghavan et al., 2005), defined as any gene-regulating activity that does not involve changes in the DNA code and is capable of persisting (Tariq and Paszkowski, 2004; Grant-Downton and Dickinson, 2005). It has become apparent that epigenetic control of transcription is mediated through specific states of chromatin structure (Exner and Hennig, 2008). Associations of DNA methylation, histone modifications and specific chromosomal proteins are involved in controlling chromatin states (Kouzarides, 2007; Pfluger and Wagner, 2007; Exner and Hennig, 2008). Epigenetic control plays an essential role in the process of cellular differentiation, allowing cells to be reprogrammed in order to generate new differentiation pathway (Valledor et al., 2007; Exner and Hennig, 2008; Meijón et al., 2008).

The regulation of the *FLOWERING LOCUS C (FLC)* in *Arabidopsis* provides a plant model of how chromatin-modifying systems have emerged as important components in the control of transition to flowering. Genetic and molecular studies have revealed three systems of *FLC* regulation: vernalization, the autonomous pathway, and *FRIGIDA (FRI)*. All these involve changes in the state of *FLC* chromatin by DNA methylation and/or histone modification (Finnegan et al., 2005; He and Amasino, 2005; Dennis and Peacock, 2007). *FLC* encodes a repressor of flowering, which is a key gene during floral transition in autonomous and vernalization pathways. Vernalization and demethylation of DNA are associated with promotion of flowering (Finnegan et al., 2000; Genger et al., 2003) and changes in histone modifications at *FLC* and its two flanking genes (Finnegan et al., 2005). In particular, for FLC repression a reduction of histone H3 acetylation and H3 trimethyl-K4, and an increase in two repression chromatin modification, histone H3 dimethyl-K9 and trimethyl-K27, at each gene in the cluster have been described, whereas histone H4 acetylation is decreased only at *FLC* (He and Amasino, 2005; Schmitz et al., 2008). The autonomous pathway also provides constitutive repression of *FLC*, and one component of this repression involves histone H3 and H4 deacetylation (He et al., 2003; Dennis and Peacock, 2007). Alternatively, *FRI* is able to overcome autonomous pathway repression and cause increased *FLC* expression. The expression of *FRI* or the loss of an autonomous pathway gene leads to increased histone H3 trimethylation at lysine 4 (He and Amasino, 2005; Kim and Michaels, 2006). This

modification is characteristic of active chromatin and *FLC* expression.

There is growing evidence that chromatin remodeling is involved in numerous processes of development and differentiation in both plants and animals (Kouzarides, 2007; Tessadori et al., 2007). DNA methylation and histone modification have been revealed as hallmarks that establish the functional status of chromatin domains (Tessadori et al., 2004) and confer the flexibility of transcriptional regulation necessary for plant development and adaptive responses to the environment (Grant-Downton and Dickinson, 2005, 2006; Vaillant and Paszkowski, 2007).

During floral transition, it is clear that gene control plays important roles, defining future tissue functions that are also linked to ornamental desirable traits such as floral quality. To achieve the new tissue structure and biochemical status, genes must be regulated plastically to be expressed only in certain cells and situations.

To test the hypothesis that the epigenetic code could be related to floral differentiation in azalea, whole DNA methylation and acetylated H4 (AcH4) levels were analyzed in vegetative and floral buds. In addition, spatial distribution of these modifications was studied by immunodetection in order to validate the results of their quantification and analyze the possible correlation between cell differentiation and heterochromatinization.

Material and methods

Plant material

Vegetative and floral buds were taken from 4-year-old azalea plants of two cultivars with different growth capacities (Blaauw's Pink with high growth and Johanna with low growth) and which demonstrated the ability to bloom under long-day conditions. Rooted cuttings of azalea were received from the Fomento Vegetal, S.A. (Castropol, Asturias, Spain) in May 2003. The plants were grown outside for 4 years in fields reserved for experimentation of SERIDA (Servicio Regional de Investigación y Desarrollo Agroalimentario de Asturias) in Villaviciosa (5°25′O, 43°28′N) (Spain) with a planting density of 3 plants/m^2 and fertirrigated three times a week with the following nutritional balances: 1-0.5-0.5 from May to July, 1-5-0 two weeks, 1-2-2 in August, and 1-1.5-3 in September and October. Each spring the plants were transplanted into bigger pots containing pinus bank as substrate, supplemented with slow release fertilizers (3.5 g/L, Basacote Plus 6M, Compo).

Buds from 20 different plants per cultivar (40 in total) were collected during spring outgrowth. Vegetative and floral buds were selected separately from the same plants and stored at −80 °C until DNA and protein extractions were performed. For immunohistochemical and histological analysis, only the Johanna cultivar was used due to anatomical similarity of buds in these cultivars.

DNA extraction

Genomic DNA was extracted from 100 mg of buds (fresh weight) using a plant genomic DNA extraction kit (DNeasy Plant Mini, Qiagen) according to the manufacturer's instructions. To prepare completely RNA-free samples, 10 μL RNase A was added (Qiagen). Finally, DNA was concentrated into DyNA Vap (Labnet of Heto) and resuspended in $_{dd}H_2O$ to a concentration of 1 μg/μL. The samples were stored at 4 °C until used.

Global DNA methylation quantification by High Performance Capillary Electrophoresis (HPCE)

For Genomic DNA hydrolysis, 5 μL DNA samples were denatured by heating for 2 min and cooling rapidly in ice. Then, 0.25 μL of 10 mM $ZnSO_4$ and 0.5 μL of nuclease P1 (Sigma; 200 U/mL in 30 mM $C_2H_3O_2Na$) were added. Mixtures were incubated for 16 h at 37 °C. Next, 0.5 μL Tris (0.5 M, pH 8.3) and 0.25 μL alkaline phosphatase [Sigma; 50 units/mL in 2.5 M $(NH_4)_2SO_4$] were added and mixtures were incubated for an additional 2 h at 37 °C. Hydrolyzed solutions were centrifuged for 20 min at 15,000*g*. Finally samples were analyzed by HPCE (CIA, Waters Chromatography) according to Fraga et al. (2002) with the modifications of Hasbún et al. (2008).

Three biological and two analytical replicates per sample were taken. Quantification of the relative methylation of each DNA sample was performed as the percentage of 5-methyldeoxycytidine (5-mdC) peak of total deoxycytidines (dC+5-mdC) peaks.

Methylation-sensitive amplification polymorphism (MSAP) analysis

The detailed protocol was adapted from Reyna-Lopez et al. (1997) and fluorescence technology was used for imaging labeled DNA fragments. The fragments were processed with ABI-PRISM 3100 DNA sequencer (Applied Biosystems) at the Sequence Analysis Service, University of Oviedo.

Restriction-ligations were done in two reactions. In the first reaction, 30 μL *HpaII* buffer 1 [5 × R/L buffer: 50 mM Tris HAc pH 7.5, 50 mM MgAc, 250 mM KAc, 25 mM dithiothreitol (DTT) 0.01% bovine serum albumin (BSA); and 5 U *Hpa*II] or 30 μL MspI buffer 1 (5 × R/L buffer and 5 U MspI) were added to 200 ng of DNA and incubated at 37 °C for 1 h. At this point, 10 μL of HpaII buffer 2 (5 × R/L buffer, 0.1 mM ATP, 5 U HpaII, 5 U EcoRI, 20 U T4 DNA ligase, 5 pM EcoRI adapter, 50 pM HpaII/MspI adapter) or MspI buffer 2 (5 × R/L buffer, 0.1 mM ATP, 5 U MspI, 5 U EcoRI, 20 U T4 DNA ligase, 5 pM EcoRI adapter, 50 pM HpaII/MspI adapter) were added, respectively, and incubated at 37 °C for 3 h. After this step, enzymes were inactivated by heating at 65 °C for 15 min.

Two consecutive PCRs were employed to selectively amplify the DNA fragments. The first PCR, pre-selective amplification, was performed adding 10 μL of 1:10 dilution of restricted-ligated DNA mixture (described above) to 20 μL of pre-selective PCR mix, giving a final concentration of 1 × PCR buffer (Invitrogen), 0.3 μM EcoRI+A primer, 0.3 μM HpaII/MspI+0 primer, 1.5 mM $MgCl_2$, 0.2 mM dNTPs and 1.5 U of Taq polymerase (Invitrogen). PCR reactions were performed in a GeneAmp 9700 (Applied Biosystems) with the following program: 94 °C for 5 min, 28 cycles of denaturing at 94 °C 30 s, annealing at 60 °C 1 min and extension at 72 °C 1 min and a final extension step of 72 °C for 15 min. After, selective amplification, the second PCR, was performed adding 5 μL of diluted pre-selective amplification to 15 μL of selective PCR mix, giving a final concentration of 1 × PCR buffer (Invitrogen), 0.3 μM EcoRI+3 primers (fluorescence labeled, Applied Biosystems) (Table 1), 0.3 μM HpaII/MspI +3 or 4 primers (Invitrogen) (Table 1), 1.5 mM $MgCl_2$, 0.2 mM dNTPs and 1 U of Taq polymerase (Invitrogen). PCR reaction program was: initial denaturing 94 °C for 5 min, 35 cycles of denaturing 94 °C 30 s, annealing 65 °C 30 s and extension 72 °C 1 min (annealing was reduced 0.7 °C/cycle for the first 12 cycles and maintained at 56 °C for the next 23 cycles) and a final extension step at 72 °C for 15 min. The different combinations of primers used are indicated in Table 1.

Table 1. Combinations of primers used.

Eco RI[a]	MspI/HpaII
AAG-JOE	AACC
AAG-JOE	CGAA
ACG-JOE	AAT
ACG-JOE	TCC
ACT-FAM	TCC
ACT-FAM	AACC
ACT-FAM	CGAA
ACT-FAM	TAGC
AAC-NED	AAT
AAC-NED	ACT
AAC-NED	TCC
AAC-NED	AACC

[a]JOE, FAM, and NED indicate the fluorocrome conjugated.

Table 2. Possible patterns of methylation changes according to Hao et al. (2004).

Change types	Change patterns[a]
De novo methylation	M+H+/M′−H′−, M+H+/M′+H′−, M+H+/M′−H′+
Demethylation	M−H−/M′+H′+, M+H−/M′+H′+, M−H+/M′+H′+
Others	M+H−/M′−H′−, M−H+/M′−H′−, M−H−\M′−H′+, M−H−\M′+H′−

[a]M and H represent the loci specific to EcoRI-MspI and EcoRI-HpaII digest, respectively, in vegetative buds. M′ and H′ represent those in the floral buds. + and − symbolize the presence and absence of DNA fragments, respectively.

Amplified fragment analysis was performed according to Rinehart (2004). In brief, peaks obtained after sequencing were analyzed using GeneMapper software to obtain the sizes of all fragments between 50 and 500 bp for each primer combination. These sizes were then translated into a binary matrix employing a specific Excel macro. The appearance–disappearance of peaks was used to study the variation of methylation in the target sequence of HpaII/MspI enzymes, which can be classified into three categories: *de novo* methylation, demethylation, and other events (Table 2). Four biological replicates per sample were analyzed and only repetitive peaks between each type of samples were considered.

Protein extraction and blot hybridization

Proteins were extracted from 250 mg of buds (fresh weight). After homogenization with liquid nitrogen using a mortar, the samples were incubated in extraction buffer 5 × [100 mM Tris, pH 8.0, 10% SDS, 5% β-mercaptoethanol, 1 mM phenylmethylsulphonylfluoride (PMSF)] for 10 min at 95 °C. Then proteins were precipitated with 5 vol of acetone containing 0.07% DTT at −20 °C. The pellet was resuspended in 1D buffer (Urea 8 M, CHAPS 2% P/V, DTT 8 Mm, glycerol 40%, trace bromophenolblue) and the proteins quantified using the Bradford assay (Bio-Rad), with ovalbumin as standard.

Proteins and standards (Low Range, Bio-RAD) were separated by electrophoresis (110 V) in 15% acrylamide SDS gels (Mini-PROTEAN II Multi-Casting

Chamber; BIO-RAD) and then transferred to Immobilon membranes (Millipore Corp., Bedford, MA) by electroblotting (350 mA for 2 h). For immunodetection, strips were blocked in a 2% dilution of powdered skimmed milk in phosphate-buffered saline (PBS) containing 0.05% Tween 20 at 4 °C overnight. Then membranes were incubated for 2 and 1 h with both primary and secondary polyclonal antibodies diluted 1/2000 and 1/1000, respectively, in the blocking solution. The primary antibodies used were anti-AcH4 polyclonal antibodies (Upstate, Cat. no. 06-866) and anti-delta-tubulin polyclonal antibodies (Chemicon, Cat. no. AB3203) as control of constitutive protein expression (Perrin et al., 2007). The secondary antibodies used were anti-rabbit IgG conjugated to alkaline phosphatase (Calbiochem, Cat. no. 401312).

Finally, the strips were washed (0.2% powdered skim milk in PBS and 0.5% Tween 20) for 5 min and the secondary antibodies revealed by treatment with a nitroblue tetrazolium, bromo-chloro-indolyl-phosphate (NBT-BCIP) mixture. Densitometric measurements were taken after immunodetection using the Kodak.1D v 3.6 Scientific Imaging Systems. Abundance index was calculated as follows: AcH4 band intensity/delta-tubulin band intensity. Four biological replicates per sample were taken.

Histological study

Vegetative and floral buds of the Johanna cultivar were sampled and fixed in 3% glutardialdehyde in phosphate buffer 0.05 M, pH 5.8 overnight at 4 °C until be used. Then, the buds were dehydrated in an ascending series of ethanol and next included in liquid paraffin. Samples were cut at 10–15 μm with a rotation microtome (Mod 1130/Biocut) and stained with 0.1% toluidine blue in phosphate buffer 0.1 M, pH 6.8. The sections were visualized using an optical microscope (Nikon Eclipse E600).

Immunohistochemical detection

Vegetative and floral buds were fixed in 4% paraformaldehyde in PBS overnight at 4 °C and stored at 4 °C in 0.1% paraformaldehyde in PBS until be used, following the procedure described by Fortes et al. (2004) with some modifications(Testillano and Risueño 2009).

The fixed buds were sectioned at 30–40 μm thickness using a cryomicrotome Leica CH 1510-1 (Leica Instruments) and were then mounted on slides coated with APTES (3-aminopropyltriethoxysilane, Sigma). The sections were permeabilized and treated with the antibodies. After the blocking reaction (5 % bovine serum albumin in PBS, for 10 min) the buds were incubated with mouse antibody anti-5-mdC (Eurogentec, Cat. no. BI-MECY-0100) or, with rabbit antibody anti-AcH4 (Upstate, Cat. no. 06-866) diluted 1/25. Alexa Fluor 488-labelled anti-mouse polyclonal antibody (Molecular Pr, Cat. no. A-11001) was used as the secondary antibody for the 5-mdC detection and Alexa Fluor 488-labelled anti-rabbit polyclonal antibody (Molecular Probes, Cat. no. 11008) for the acetylated H4 histone detection. Finally the slides were counterstained with DAPI (4',6-diamidino-2-phenylindole; Fluka). In both immunochemical detection (5-mdC and AcH4) the negative controls were obtained replacing the primary antibody with PBS.

Fluorescence was visualized using a confocal microscope (Leica TCS-SP2-AOBS) connected to a workstation and the images were processed with Leica Software (LCS 2.5).

In addition to data obtained by confocal microscopy, each image was divided into multiple fields and relative rates of DNA methylation (MI) and acetylation of histone H4 (AI) were calculated as follows:

$$MI(\%) = \textit{Nuclei with}\ \text{5-mdC signal} \times 100/\text{Nuclei stained with DAPI}$$

$$AI(\%) = \text{Nuclei with AcH4 signal} \times 100/\text{Nuclei stained with DAPI}$$

Statistical analysis

The data for global methylation and quantification of AcH4 were analyzed using SigmaStat 3.1.

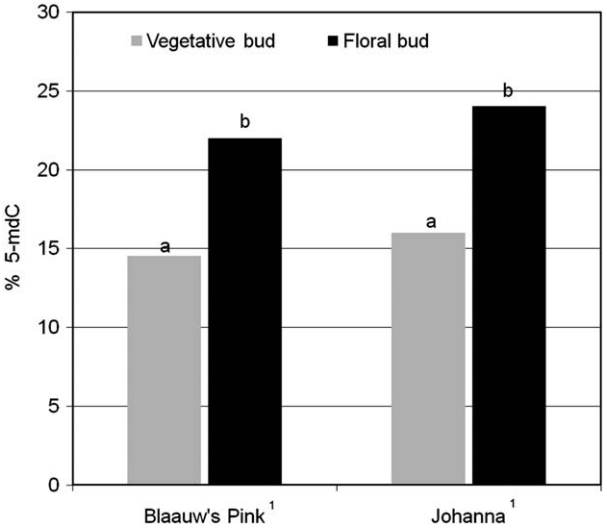

Figure 1. Percentage of 5-methylcytosine in vegetative and floral buds of Blaauw's Pink and Johanna cultivars. Within each cultivar, different letters indicate significant differences ($p \leqslant 0.001$; $n = 3$) while between cultivars different numbers show significant differences ($p \leqslant 0.001$; $n = 3$).

software. In both cases, a two-way ANOVA (analysis of variance) (cultivar and type of bud) was used, with cultivar as the main factor.

Results

DNA methylation

Global DNA methylation (quantification by HPCE)

Vegetative buds showed significantly lower levels of 5-mdC than floral buds in both cultivars, reaching a value of approximately 16% in Johanna and 15% in Blaauw's Pink (Figure 1). Conversely, floral buds presented values of methylation of about 24% in Johanna and 22% in Blaauw's Pink. The statistical analyses did not show significant differences between cultivars ($n = 3$, $p \leqslant 0.001$); however, Johanna always showed, in both buds, higher levels of 5-mdC than did Blaauw's Pink.

MSAP analysis

Additional analysis of CCGG sequence-specific DNA methylation patterns, performed by MSAP, showed that the transition between vegetative and floral buds also occurred with changes in the MSAP fragment patterns in both cultivars. The primer combinations used generated a total of 664 loci, of which 27.2% in Johanna, and 31.7% in Blaauw's Pink were monomorphic, the rest being polymorphic (206 in Johanna and 188 in Blaauw's Pink) (Table 3) associated with different status of cytosine methylation sites or to events of unknown nature.

In the *Eco*RI-*Msp*I digests, 29 events, in Johanna and 44 in Blaauw's Pink appeared specific, which means that the internal cytosine of the recognition site remains methylated during floral differentiation in these fragments. Alternatively, 35 events in Johanna, and 32 in Blaauw's Pink, were exclusive for the *Eco*RI-*Hpa*II digests, indicating that these sites keep the external cytosine methylated in one of the strands at

Table 3. DNA methylation changes during floral transition in Johanna and Blaauw's Pink cultivars.

Primer combinations	Specific E-M[a]	Specific E-H[a]	*de novo*[b] methylation	Demethylation[b]	Others	Loci monomorphism (%)	Total loci
Johanna							
AAC AACC	8	8	17	12	28	25 (25.5%)	98
AAC AAT	1	1	19	2	26	16 (24.6%)	65
AAC ACT	0	5	7	2	9	9 (28%)	32
AAC TCC	3	4	14	7	28	27 (32%)	83
AAG AACC	0	3	29	4	32	6 (8%)	74
AAG CGAA	6	2	12	3	13	1 (28%)	50
ACG AAT	5	1	6	2	11	4 (14%)	29
ACG TCC	2	3	11	0	15	22 (41.5%)	53
ACT AACC	2	4	10	9	9	19 (36%)	53
ACT CGAA	1	1	10	2	2	14 (46.6%)	30
ACT TAGC	0	1	8	6	19	19 (35.8%)	53
ACT TCC	1	2	18	3	14	6 (14%)	44
Total	29	35	161	52	206	181 (27.2%)	664
Blaauw's Pink							
AAC AACC	14	5	17	8	24	30 (30%)	98
AAC AAT	1	2	19	1	25	17 (26%)	65
AAC ACT	0	6	4	3	8	11 (34%)	32
AAC TCC	5	2	12	10	22	32 (38%)	83
AAG AACC	0	4	18	6	26	20 (27%)	74
AAG CGAA	8	1	12	3	18	8 (16%)	50
ACG AAT	6	1	4	2	8	8 (27%)	29
ACG TCC	3	4	14	4	12	16 (30%)	53
ACT AACC	1	1	10	8	10	23 (43.4%)	53
ACT CGAA	0	1	8	1	6	14 (46.6%)	30
ACT TAGC	3	2	8	3	13	24 (45.3%)	53
ACT TCC	2	4	11	3	16	8 (18.2%)	44
Total	44	32	132	52	118	221 (31.7%)	664

The percentage of monomorphism was calculated as the number of monomorphic loci of the total of detected loci.
[a]E-M and E-H indicate specific digestions of *Eco RI-Msp I* and *Eco RI-Hpa II*, respectively.
[b]The events of *de novo* methylation and demethylation were detected in floral buds compared with vegetative buds.

the recognition sites. A total of 161 and 137 changes in the methylation patterns were ascribed to *de novo* methylation process in Johanna and Blaauw's Pink, respectively. However, only 52 demethylation events were observed in both cultivars.

Quantification of AcH4

Protein extracts from vegetative and floral buds of both cultivars revealed single bands of approximately 15 and 35 kDa for AcH4 and tubulin, respectively (Figure 2). The abundance index of AcH4 in vegetative buds reached high values of 0.85 ± 0.012 in Johanna and 0.79 ± 0.012 in Blaauw's Pink, while that in floral buds decreased to 0.65 ± 0.012 in Johanna and 0.67 ± 0.09 in Blaauw's Pink. Statistically significant differences were observed between types of buds and cultivars ($n = 4$, $p \leqslant 0.001$).

Micromorphological study of vegetative and floral buds

Morphological and histological study

In vegetative bud (Figure 3A–C) leaf primordial, axillary buds procambium and SAM were clearly observed. The SAM was made up of two cell populations with distinct morphology and behavior (Figure 3D): the central cells (corpus), larger and more rounded, that remain pluripotent and the apical dome, large number of smaller cells (tunica) that contribute to organ formation and eventually differentiate. In floral buds (Figure 3E–H), differentiated parts of flower were already apparent (sepals, petals, etc.).

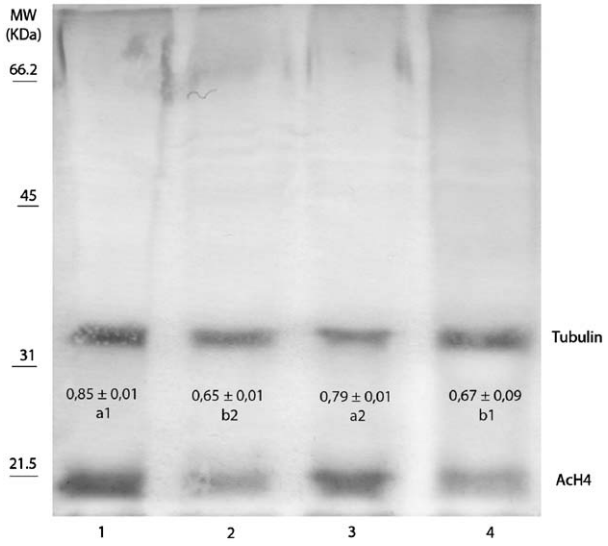

Figure 2. Analysis of AcH4 and tubulin in vegetative and floral buds by immunoblotting. (The figure shows a representative membrane.) Average values of abundance index of AcH4 ($\pm$SE). Lane 1: tubulin and AcH4 in vegetative bud of Johanna; Lane 2: tubulin and AcH4 in floral bud of Johanna; Lane 3: tubulin and AcH4 in vegetative bud of Blaauw's Pink; Lane 4: tubulin and AcH4 in floral bud of Blaauw's Pink. Marker bands are indicated to the left of the blot. Within each cultivar, different letters indicate significant differences ($p \leqslant 0.001$; $n = 4$) while within each type of bud different numbers indicate significant differences ($p \leqslant 0.001$; $n = 4$).

Immunohistochemical detection of 5-mdC and AcH4

Distribution of 5-mdC in vegetative buds was localized mainly in the apical dome, leaf primordial and procambium (Figure 4A–H), reaching 200 units of fluorescence intensity and values of 90% of IM in the cells of the apical dome (tunica) (Figure 5A–C). A lower 5-mdC signal was detected in the central cells of SAM (corpus), 50 units of fluorescence intensity and 30% of IM (Figure 5A–C). In vegetative buds, the apical dome, leaf primordial and procambium were also strongly stained with DAPI, indicating elevated number of cells and heterochromatization (Figure 4C and G). On the other hand, in floral buds, more intense florescence marking of 5-mdC was observed, mostly localized in the differentiated parts of flower: sepals, petals and surrounding tissues, all also intensely stained with DAPI (Figure 4I–L). The differentiated tissue showed fluorescence levels of 250 units and IM of 100%, while the poorly differentiated tissue presented lower fluorescence levels, reaching a maximum of 50 units and IM of 25% (Figure 5D–F).

The immunolocalization of AcH4 showed an opposite layout relative to 5-mdC and DAPI. In vegetative buds, the AcH4 signal was lower in the apical dome (Figure 4M–T), gradually increasing approaching the meristem base and reaching the maximum marker intensity (about 150 fluorescence units and an IA of 80%) in the central cells of SAM (corpus) (Figure 5G–I). The floral buds showed a low AcH4 signal (Figure 4U–X), reaching a maximum of 50 fluorescence units and 30% of IA in the poorly differentiated tissue, while the differentiated tissue showed an even lower fluorescence signal (10 fluorescence units and 10% of IA) (Figure 5J–L).

Discussion

The experimental results showed that both HPCE and MSAP methods revealed an increase in global DNA methylation from the vegetative to flowering stage.

The quantification of 5-mdC by HPCE showed similar methylation patterns in both cultivars, with

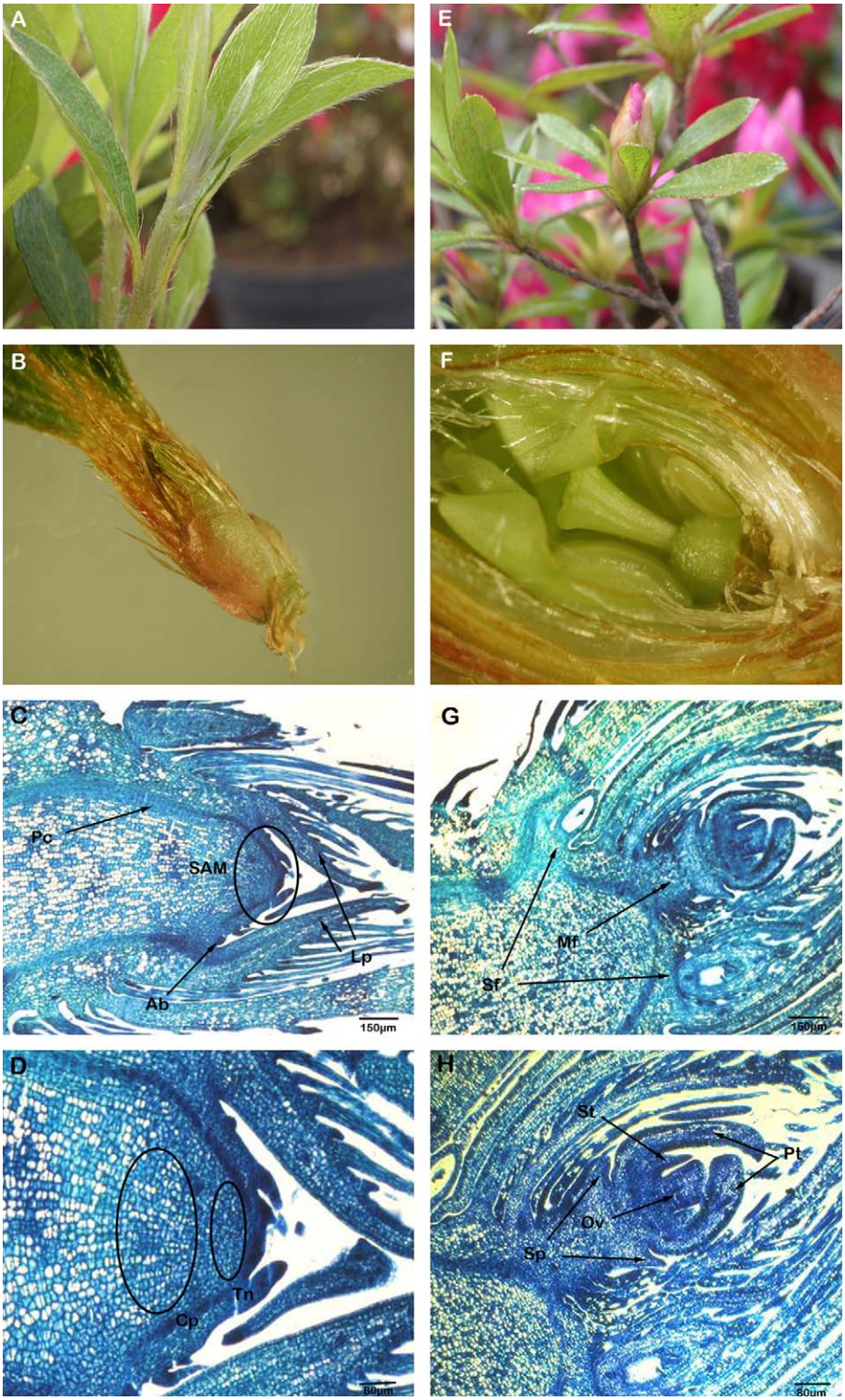

Figure 3. Morphological and histological structure of Johanna cultivar buds (longitudinal image and sections): (A) vegetative shoot, (B) vegetative shoot under stereomicroscope, (C) vegetative bud under optical microscope (10 ×), (D) vegetative bud optical microscope (20 ×), (E) floral shoot, (F) floral shoot under stereomicroscope, (G) floral bud optical microscope (10 ×) and (H) floral bud optical microscope (20 ×). Abbreviations: Pc = procambium, SAM = shoot apical meristem, Lp = leaf primordial, Ab = axillary bud, Sf = secondary flower, Mf = main flower, Cp = corpus, Tn = tunica, Sp = sepals, St = stamen, Ov = ovule, Pt = petals.

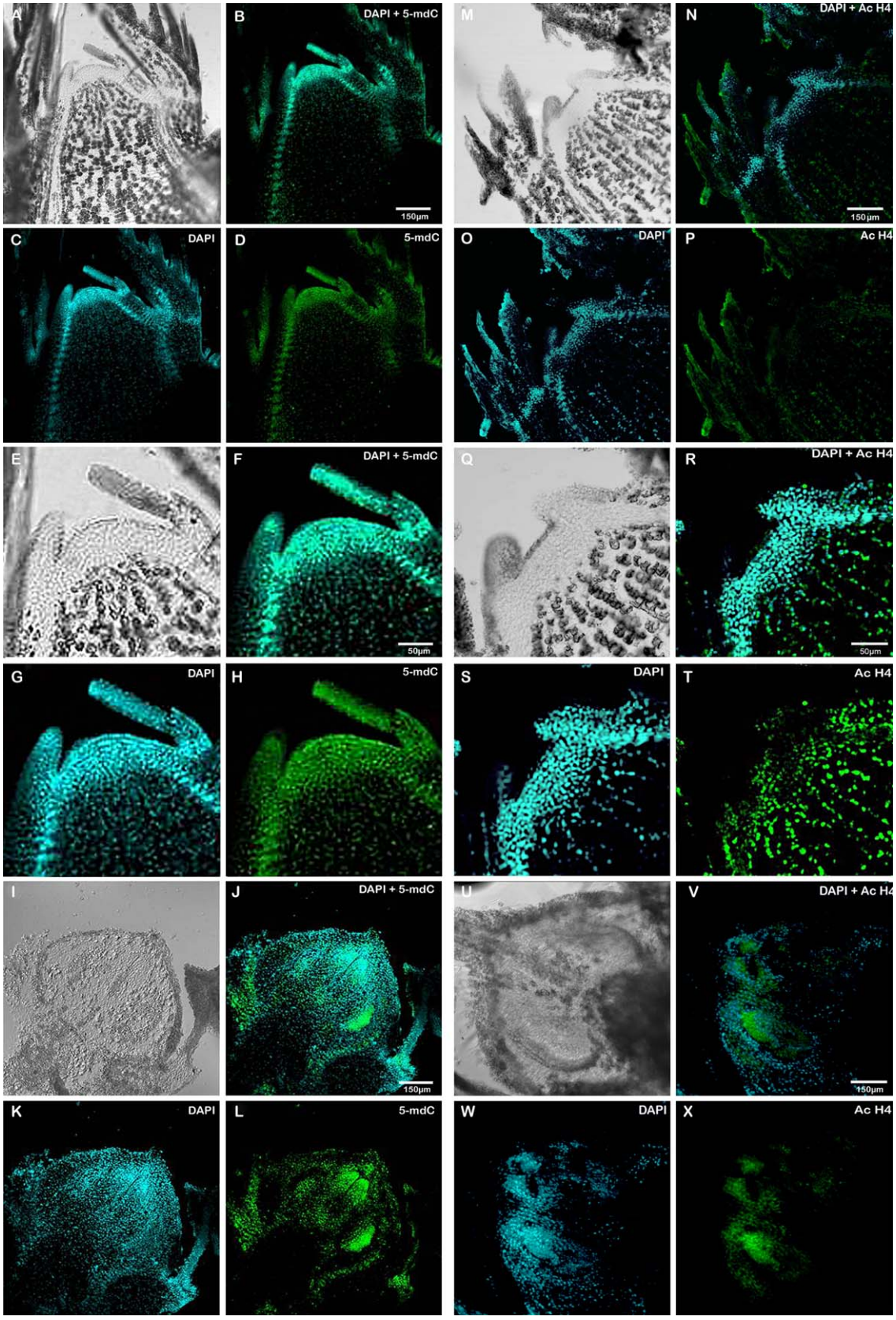
A
B
DAPI + 5-mdC
150µm
M
N
DAPI + Ac H4
150µm
C
DAPI
D
5-mdC
O
DAPI
P
Ac H4
E
F
DAPI + 5-mdC
50µm
Q
R
DAPI + Ac H4
50µm
G
DAPI
H
5-mdC
S
DAPI
T
Ac H4
I
J
DAPI + 5-mdC
150µm
U
V
DAPI + Ac H4
150µm
K
DAPI
L
5-mdC
W
DAPI
X
Ac H4

the vegetative bud values around 10% lower than the floral buds. On the other hand, Johanna cultivars reached higher levels of global methylation and a larger number of *de novo* methylation events than Blaauw's Pink. This may be linked to the different development pattern of each cultivar, as Blaauw's Pink presents major growth and a more robust architecture than Johanna, requiring it to have a more dynamic metabolism and higher levels of gene expression. According to Hasbún et al. (2007), the apical meristems of juvenile individuals show great morphogenic ability and growth associated with low levels of DNA methylation. However, the mature individuals with less morphogenic ability showed higher levels of DNA methylation.

Moreover, MSAP analysis showed that, although mostly *de novo* methylation events occur during floral development, demethylation events are also generated. In contrast to *de novo* methylation, both cultivars presented the same number of demethylation events, indicating that these species exhibit high conservation in demethylation processes, largely linked to gene activation during the floral transition (Finnegan et al., 2000; Genger et al.,2003). The survival of the species depends on the success of floral development (Blázquez and Weigel, 2000) and, perhaps this fact is responsible for maintaining the number of demethylation events in both cultivars and is probably associated with the activation of specific genes involved in the floral transition.

Furthermore, wide variation in the distribution of 5-mdC was found within different tissues of SAM and between the two stages of bud development by immunolocalization. In vegetative buds, the cells of the peripheral zone showed a higher 5-mdC signal and degree of differentiation and heterochromatinization, whereas the cells of the central zone remained pluripotent, presenting lower levels of 5-mdC and DAPI labeling. In floral buds, this zonation pattern was lost and the 5-mdC was localized in the different parts of the flower. The distribution of 5-mdC revealed by immunolocalization studies is in agreement with the results of Zluvova et al. (2001) concerning DNA methylation and replication patterns during SAM development. These authors suggested that the mature vegetative apex is characterized by the zonation model: the very slowly dividing central zone is surrounded by the peripheral zone with a higher DNA division rate. After the transition to flowering, cell division in the SAM is restored. The DNA replication pattern in SAM negatively correlates with the DNA methylation pattern, i.e. the high division ratio corresponds with low DNA methylation. On the other hand, Ruiz-García et al. (2005) also observed that, in *Arabidopsis* development, a progressive DNA methylation trend from cotyledons to vegetative organs to reproductive organs. According to these results, the central zone of the SAM in the vegetative stage can represent a relatively quiescent "stem-line" that is activated after the floral transition for developing different parts of the flower.

DNA methylation plays an essential role in plant development as a mechanism to epigenetically maintain developmental decisions in proliferating and differentiating cells (Vanyushin, 2006; Hasbún et al., 2007; Valledor et al., 2007; Berdasco et al., 2008). However, other epigenetic chromatin modifications, such as histone modification, also seem to be connected (Loidl, 2004; Pfluger and Wagner, 2007; Berdasco et al., 2008).

Our results showed high values of AcH4 in vegetative buds. However, after the floral transition, in floral buds, the values of AcH4 decreased considerably. This appears to be in agreement with data from DNA methylation studies and the assumption of the loss of gene activity during the meristem differentiation, in this case, during the floral transition. Histone modification provides an additional level of regulation of gene expression

Figure 4. Immunodetection of 5-mdC and AcH4 in sections of vegetative and floral buds of Johanna in longitudinal axis using a confocal microscope: (A) differential interference contrast (DIC) of vegetative bud (10 ×), (B) DAPI (blue signals) superposition and 5-mdC (green signals) of vegetative bud (10 ×), (C) DAPI labeling of nuclei of vegetative bud (10 ×), (D) 5-mdC labeling of vegetative bud (10 ×), (E) DIC of vegetative bud (40 ×), (F) DAPI (blue signals) superposition and 5-mdC (green signals) of vegetative bud (40 ×), (G) DAPI labeling of nuclei (40 ×), (H) 5-mdC labeling of vegetative bud (40 ×), (I) DIC of floral bud (20 ×), (J) DAPI (blue signals) superposition and 5-mdC (green signals) of floral bud (20 ×), (K) DAPI labeling of nuclei of floral bud (20 ×), (L) 5-mdC labeling of floral bud (20 ×), (M) DIC of vegetative bud (10 ×), (N) DAPI (blue signals) superposition and AcH4 (green signals) of vegetative bud (10 ×), (O) DAPI labeling of nuclei of vegetative bud (10 ×), (P) AcH4 labeling of vegetative bud (10 ×), (Q) DIC of vegetative bud (40 ×), (R) DAPI (blue signals) superposition and AcH4 (green signals) of vegetative bud (40 ×), (S) DAPI labeling of nuclei (40 ×), (T) AcH4 labeling of vegetative bud (40 ×), (I) DIC of floral bud (20 ×), (J) DAPI (blue signals) superposition and AcH4 (green signals) of floral bud (20 ×), (K) DAPI labeling of nuclei of floral bud (20 ×) and (L) AcH4 labeling of floral bud (20 ×). (For interpretation of the references to color in this figure legend, the reader is referred to the web version of this article.)

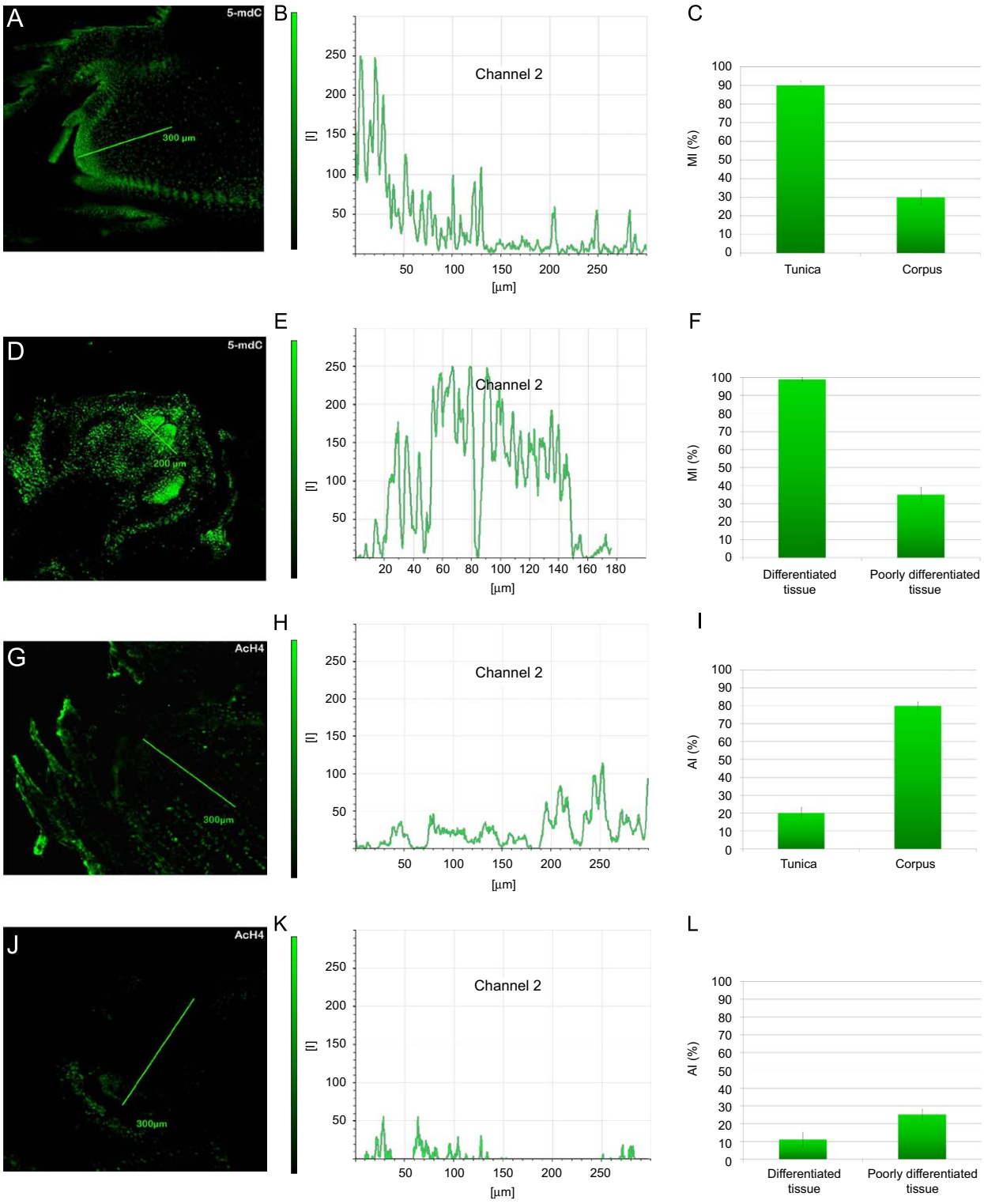

Figure 5. Intensity of 5-mdC and AcH4 fluorescence markers in vegetative and floral buds: (A) 5-mdC labeling of vegetative bud (10 ×), (B) intensity of 5-mdC fluorescence markers along the line shown in the vegetative bud, (C) average of methylation index (MI) in tunica and corpus of vegetative bud (±SE), (D) 5-mdC labeling of floral bud (10 ×), (E) intensity of 5-mdC fluorescence markers along the line shown in the floral bud, (F) average of MI in differentiated tissue and poorly differentiated tissue of floral bud (±SE), (G) AcH4 labeling of vegetative bud (10 ×), (H) intensity of AcH4 fluorescence mark along the line shown in the vegetative bud, (I) average of acetylation index (AI) in tunica and corpus of vegetative bud (±SE), (J) AcH4 labeling of floral bud (20 ×), (K) intensity of AcH4 fluorescence marker along the line shown in the vegetative bud, (L) average of AI in differentiated tissue and poorly differentiated tissue of floral bud (±SE).

beyond that of DNA methylation and the transcription factors that recruit RNA polymerase to target genes (Reyes, 2006; Vaillant and Paszkowski, 2007).

The distribution of AcH4 presented an opposite pattern relative to 5-mdC. Apical meristems, during vegetative growth, and particularly regions with a high degree of differentiation and heterochromatinization such as the apical dome, leaf primordial, and the vascular bundle, showed a low signal for AcH4, with the central zone of SAM having higher levels of AcH4 labeling. Conversely, in the floral bud, an AcH4 signal was barely detected. These results are in concordance with the SAM zonation model during vegetative growth (Zluvova et al., 2001) and confirm that DNA methylation and histone H4 deacetylation are factors involved in the complex gene regulation responsible for floral differentiation and heterochromatinization (Tessadori et al., 2007).

The expression level of a gene is determined not only by sequence-specific regulatory factors, but also by a complex network of co-acting proteins. Many of these proteins directly or indirectly affect the structure of the chromatin environment in which the gene is embedded. Recent studies of histones and DNA modification support and refine the concept of the chromatin environment being key to the establishment and maintenance of transcriptional activity or repression (Loidl, 2004; Reyes, 2006; Vaillant and Paszkowski, 2007). Histone modification and DNA methylation can activate or repress transcription by generating ''open'' or ''closed'' chromatin configurations, respectively. Generally, open chromatin increases the accessibility of the genome to transcription machinery, while closed chromatin represses gene expression by limiting the accessibility (Reyes, 2006; Kouzarides, 2007; Pfluger and Wagner, 2007). The acetylation of specific lysine residues within the amino-terminal tails of H3 and H4 and DNA demethylation are positively correlated with open chromatin configuration and gene activity in meristematic tissue of plants (Law and Suttle, 2005), and both epigenetic processes are connected by particular molecular routes (Loidl, 2004; Pfluger and Wagner, 2007).

In this study, we demonstrate large-scale reorganization of chromatin by local changes in DNA methylation and histone H4 acetylation in vegetative and floral buds of azalea. Chromatin states change during plant development. Globally, cytologically defined heterochromatin increases during cell differentiation and organ maturation, while it decreases during cell de-differentiation and reorganization process (Tessadori et al., 2007; Exner and Hennig, 2008).

In summary, the floral transition in plants is a complex process and epigenetic control and reorganization of chromatin seems to be determinative for coordinating floral development in azalea. The results of this work indicate that DNA methylation and deacetylation of histone H4 are not static and that both epigenetic mechanisms have particular dynamics in vegetative and floral states of SAM. These mechanisms act simultaneously and in coordination, restructuring the chromatin and regulating the gene expression in SAM development and floral differentiation.

Acknowledgements

This research was supported by funds from the Spanish Ministry of Science and Technology (projects AGL 2004-00810 and AGL2007-62907/FOR). The Spanish I.N.I.A. supported the fellowship of Mónica Meijón. Fomento Vegetal S.A. (Castropol, Asturias, Spain) for providing the plant material.

References

Araki T. Transition from vegetative to reproductive phase. Current Opinion in Plant Biology 2001;4:63–8.

Berdasco M, Alcázar R, García-Ortiz MV, Ballestar E, Fernández AF, Roldán-Arjona T, et al. Promoter DNA hypermethylation and gene repression in undifferentiated *Arabidopsis* cells. PLoS ONE 2008;3:3306.

Blázquez MA, Weigel D. Integration of floral inductive signals in Arabidopsis. Nature 2000;404:889–92.

Bodson M. Effect of photoperiod and irradiance on floral development of young plants of a semi-early and a late cultivar azalea. Journal of American Society of Horticulturae Science 1983;108:382–6.

Dennis ES, Peacock WJ. Epigenetic regulation of flowering. Current Opinion in Plant Biology 2007;10:520–7.

Exner V, Hennig L. Chromatin rearrangements in development. Current Opinion in Plant Biology 2008;11:64–9.

Finnegan EJ, Peacock WJ, Dennis ES. DNA methylation, a key regulator of plant development and other processes. Current Opinion in Genetics and Development 2000;10:217–23.

Finnegan EJ, Kovac KA, Jaligot E, Sheldon CC, Peacock WJ, Dennis ES. The downregulation of FLOWERING LOCUS C (FLC) expression in plants with low levels of DNA methylation and by vernalization occurs by distinct mechanisms. The Plant Journal 2005;44:420–32.

Fortes AM, Coronado MJ, Testillano PS, Risueño MC, Pais MS. Expresión of lipoxygenase during organogenic nodule formation from hop internotes. Journal of Histochemistry and Cytochemistry 2004;52:227–41.

Fraga MF, Uriol E, Diego LB, Berdasco M, Esteller M, Cañal MJ, et al. High-performance capillary electrophoretic method for the quantification of 5-methyl 2′-deoxycytidine in genomic DNA: application to plant, animal and human cancer tissues. Electrophoresis 2002;23:1677–81.

Genger RK, Peacock WJ, Dennis ES, Finnegan EJ. Opposing effect of reduced DNA methylation on flowering time in *Arabidopsis thaliana*. Planta 2003;216:461–6.

Grant-Downton RT, Dickinson HG. Epigenetic and its implications for plant biology 1. The epigenetic network in plants. Annals of Botany 2005;96:1143–64.

Grant-Downton RT, Dickinson HG. Epigenetic and its implications for plant biology 2. ''The epigenetic epiphany'': Epigentics, evolution and beyond. Annals of Botany 2006;97:11–27.

Hao Y-J, Wen X-P, Deng X-X. Genetic and epigenetic evaluations of citrus calluses recovered from slow-growth culture. Journal of Plant Physiology 2004;161: 479–84.

Hasbún R, Valledor L, Berdasco M, Santamaría E, Cañal MJ, Rodríguez R. Dynamics of DNA methylation in chestnut trees development. Acta Horticulturae 2007;760:563–6.

Hasbún R, Valledor L, Rodríguez JL, Santamaría E, Ríos D, Sanchez M, Cañal MJ, Rodríguez R. HPCE quantification of 5-methyl-2′-deoxycytidine in genomic DNA: methodological optimization for chestnut and other woody species. Plant Physiology and Biochemistry 2008;46:815–22.

He Y, Amasino RM. Role of chromatin modification in flowering-time control. Trends in Plant Science 2005; 10:30–5.

He Y, Michaels SD, Amasino RM. Regulation of flowering time by histone acetylation en *Arabidopsis*. Science 2003;302:1751–4.

Henderson IR, Dean C. Control of Arabidopsis flowering: the chill before the bloom. Development 2004;131:3829–38.

Jacqmard A, Gadisseur I, Bernier G. Cell division and morphological changes in the shoot apex of Arabidopsis thaliana during floral transition. Annals of Botany 2003;91:571–6.

Kim SY, Michaels SD. SUPPRESSOR OF FRI 4 encodes a nuclear localized protein that is required for delayed flowering in winter-annual *Arabidopsis*. Development 2006;133:4699–707.

Kouzarides T. Chromatin modification and their function. Cell 2007;128:693–705.44.

Law RD, Suttle JC. Chromatin remodelling in plant cell culture: patterns of DNA methylation and histone H3 and H4 acetylation vary during growth of asynchronous potato cell suspensions. Plant Physiology and Biochemistry 2005;43:527–34.

Loidl P. A plant dialect of the histone language. Trend in Plant Science 2004;9:84–90.

Meijón M, Valledor L, Rodríguez JL, Hasbún R, Santamaría E, Feito I, et al. Plant Epigenetics. In: Esteller M, editor. Epigenetics in biology and medicine. Boca Raton, FL: CRC Press; 2008. p. 225–40.

Meijón M, Rodriguez R, Cañal MJ, Feito I. Improvement of compactness and floral quality in azalea by means of application of plant growth regulators. Scientia Horticulturae 2009;119:169–76.

Perrin RM, Wang Y, Christen YL, Wil J, Masson PH. WVD2 is a novel microtubule-associated protein in *Arabidopsis thaliana*. The Plant Journal 2007;49:961–71.

Pfluger J, Wagner D. Histone modification and dynamic regulation of genome accessibility in plants. Current Opinion in Plant Biology 2007;10:645–52.

Reyes JC. Chromatin modifiers that control plant development. Current Opinion in Plant Biology 2006;9:21–7.

Reyna-Lopez GE, Simpson J, Ruiz-Herrera J. Differences in DNA methylation patterns are detectable during the dimorphic transition of fungi by amplification of restriction polymorphisms. Molecular Genetics and Genomics 1997;253:703–10.

Rinehart TA. AFLP analysis GeneMapper software and Excel macro that aligns and converts output to binary. BioTechniques 2004;37:186–8.

Ruiz-García L, Cervera MT, Martínez-Zapater JM. DNA methylation increases throughout *Arabidopsis* development. Planta 2005;222:301–6.

Schmitz RJ, Sung S, Amasino RM. Histone arginine methylation is required for vernalization-induced epigenetic silencing of FLC in winter-annual *Arabidopsis thaliana*. Proceedings of the National Academy of Science USA 2008;105:411–6.

Tariq M, Paszkowski J. DNA and histone methylation in plants. TREND in Genetics 2004;20:244–51.

Tessadori F, Van Driel R, Fransz P. Cytogenetics as a tool to study gene regulation. Trend in Plant Science 2004;9: 147–53.

Tessadori F, Kees Schulkes R, Van Driel R, Fransz P. Light-regulated large-scale reorganization of chromatin during the floral transition in Arabidopsis. The Plant Journal 2007;50:848–57.

Testillano PS, Risueño MC. Tracking gene and protein expression during microspore embryogenesis by confocal laser scanning microscopy. In: Touraev A, et al. editors. Advances in haploid production in higher plants. Heidelberg: Springer Verlag; 2009. p. 339–47.

Tooke F, Battey N. Models of shoot apical meristem function. New Phytologist 2003;159:37–52.

Vaillant I, Paszkowski J. Role of histone and DNA methylation in gene regulation. Current Opinion in Plant Biology 2007;10:528–33.

Valledor L, Hasbun R, Meijón M, Rodríguez JL, Santamaría E, Viejo M, et al. Involvement of DNA methylation in tree development and micropropagation. Plant Cell Tissue and Organ Culture 2007;91:75–86.

Vanyushin BF. DNA methylation in plants. Current Topics in Microbiology and Immunology 2006;301:67–122.

Vijayraghavan U, Prasad K, Meyerowitz E. Specification and maintenance of the floral meristem: interactions between positively-acting promoters of flowering and negative regulators. Current Science 2005;89:1835–43.

Zluvova J, Janousek B, Vyskot B. Immunohistochemical study of DNA methylation dynamics during plant development. Journal of Experimental Botany 2001;365:2265–73.